Veterinary Immunology and Immunopathology 134 (2010) 230–238

Contents lists available at ScienceDirect

Veterinary Immunology and Immunopathology

journal homepage: www.elsevier.com/locate/vetimm

Research paper

Identification of functional domains of chicken Interleukin 2

Jianyou Gu [a,b], Xizhen Ruan [a,b], Zhenyu Huang [a,b], Jigang Chen [a], Jiyong Zhou [a,b,*]

[a] Key Laboratory of Animal Epidemic Etiology & Immunological Prevention of Ministry of Agriculture, Zhejiang University, Hangzhou 310029, PR China
[b] State Key Laboratory for Diagnosis and Treatment of Infectious Diseases, The First Affiliated Hospital, Zhejiang University, Hangzhou 310003, PR China

ARTICLE INFO

Article history:
Received 9 May 2009
Received in revised form 5 October 2009
Accepted 13 October 2009

Keywords:
Chicken interleukin 2
Functional domain
Tertiary structure

ABSTRACT

Interleukin 2 (IL-2) is an essential cytokine that plays a pivotal role in the replication, maturation and differentiation of lymphocytes. In this study, the functional domains of chicken IL-2 (chIL-2) were mapped with monoclonal antibodies (mAb), a synthetic peptide, and a phage display peptide library. Nine neutralizing mAbs to chIL-2 were produced using the recombinant chIL-2 monomer expressed in prokaryotic cells as an immunogen and used to finely map the functional domains of the chIL-2 protein. The mimotopes of nine anti-chIL-2 mAbs, including KIELPSL, EHLDXNDSLYL, NHLXGXY, WHLPPSL, EFKASXL, TENPFPE, SGLYL, AHGYWEL and HHGYWEL, were respectively identified by phage display and peptide-competitive ELISA. These mimotopes constitute three conformational functional domains in the chIL-2 molecule, that is, $N^{26}K^{27}I^{28}H^{29}L^{30}E^{31}L^{32}P^{35}Q^{43}Q^{44}T^{45}L^{46}Q^{47}C^{48}Y^{49}L^{50}$ (domain I), $E^{68}E^{69}F^{70}K^{79}K^{82}S^{83}L^{84}T^{85}G^{86}L^{87}$ (domain II) and $N^{88}H^{89}G^{91}K^{104}F^{105}P^{106}D^{107}E^{111}L^{112}Y^{118}L^{119}$ (domain III). The neutralizing mAbs to chIL-2 inhibited the in vitro lymphocyte proliferation stimulated by three peptide domains of chIL-2. The predicted tertiary structure of chIL-2 reveals that domain I was positioned in the long A–B loop and the N terminal of Helix B, domain II was mostly situated in Helix C, and domain III was distributed in the C–D loop and Helix D. These data demonstrate the functional domains of chIL-2 and provide a clue for elucidating the interaction between chIL-2 and its receptor.

1. Introduction

Interleukin 2 (IL-2) is an essential cytokine secreted mainly by activated T lymphocytes and plays a pivotal role in the replication and differentiation of T and B lymphocytes, monocytes, and natural killer cells (Rubin, 1995). The important immunoregulatory role of IL-2, as well as the therapeutic prospects it holds for the treatment of certain cancers and infectious diseases, has made it the focus of numerous structure–function studies (Farner et al., 1997). The first mutational analysis of mouse IL-2 identified the N terminal region between amino acids 14 and 37 as a region important for biological activity (Zurawski et al., 1986). Functional domains of human IL-2 were subsequently identified using oligonucleotide-directed mutagenesis, which indicated that the N terminal 20 amino acids, the C terminal 13 amino acids, and two of three cysteine residues must be retained for bioactivity (Ju et al., 1987). The study of IL-2 analogs was subsequently expanded to identify the specific amino acid residues required for binding to IL-2 receptor (IL-2R) subunits. The D^{20} substitution in IL-2 abolished binding to the receptor beta chain (Collins et al., 1988). The epitope mapping of a monoclonal antibody (mAb) re-affirmed the interaction between D^{20} and the IL-2R beta chain (Eckenberg et al., 1997). Amino acid Q^{126} in human IL-2 and Q^{141} in mouse IL-2 were found to be the critical amino acid for binding

* Corresponding author at: Key Laboratory of Animal Epidemic Etiology & Immunological Prevention of Ministry of Agriculture, Zhejiang University, 268 Kaixuan Road, Hangzhou, Zhejiang 310029, PR China. Tel.: +86 571 8697 1698; fax: +86 571 8697 1821.
E-mail address: jyzhou@zju.edu.cn (J. Zhou).

0165-2427/$ – see front matter © 2009 Elsevier B.V. All rights reserved.
doi:10.1016/j.vetimm.2009.10.021

with IL-2R gamma chain (Buchli and Ciardelli, 1993). The quaternary ectodomain complex of IL-2 with IL-2R alpha, beta, and gamma receptors was constructed by crystallization, and the interactive contact sites were displayed. The binding of IL-2R alpha chain to IL-2 stabilized a secondary binding site for presentation to IL-2R beta chain, and IL-2R gamma chain was recruited to the composite surface formed by the IL-2/IL-2R beta complex (Wang et al., 2005a).

Since Sundick and Gill-Dixon (1997) cloned the chicken IL-2 (chIL-2) gene, the duck and goose IL-2 genes and their receptor genes have been cloned and characterized as well (Zhou et al., 2005a,b; Teng et al., 2006; Wang et al., 2007; Gu et al., 2007). ChIL-2 plays an important role in the replication and maturation of T lymphocytes (Hilton et al., 2002) and natural killer cells (Choi and Lillehoj, 2000). It has been used to improve the vaccines response to *Eimeria* parasites (Xu et al., 2008) and infectious bursal disease virus (Hulse and Romero, 2004), indicating that chIL-2 potentially has a practical importance in enhancing immune responses to vaccines. Despite this, studies on chIL-2 functional domains have thus far been scarce. In the present study, we sought to determine the functional domains of chIL-2 using epitope mapping and bioactive identification.

2. Materials and methods

2.1. Cells

COS-7 cells were maintained in RPMI-1640 medium (Gibco BRL, Gaithersburg, MD) supplemented with 10% newborn calf serum. Splenic mononuclear cells (SMC) were prepared as described previously (Zhou et al., 2003).

2.2. Preparation of recombinant soluble chIL-2

The chIL-2 ORF, without the signal peptide sequence, was obtained by polymerase chain reaction (PCR) using the following primers: forward primer 5′-TACCATGGCATCTC-TATCATCAGAAAAA-3′, containing the NcoI site, and reverse primer 5′-GT*GCGGCCGC*TTAATGATGATGATGAT-GATGTTTTTGCAGATATCTCAC-3′, containing the NotI site. The PCR product of chIL-2, with a His tag at the C-terminus, was cloned into the pET28a (+) vector (Merck KGaA, Darmstadt, Germany). The resulting plasmid was designated as pET28a-chIL-2. *E. coli* strain BL21 (DE3) was then transformed with the vector pET28a-chIL-2 and incubated at 37 °C in LB broth. When the optical density (OD_{600}) reached 1.8, 0.01 mM isopropyl-1-thio-L-D-galactopyranoside (IPTG) was added to induce protein expression. Recombinant chIL-2 protein (rchIL-2) was purified by a nickel column under native conditions following the manufacturer's instructions (Qiagen Inc., Valencia, CA). The rchIL-2 protein monomer was further isolated using a HiLoad 26/60 Superdex 75 prep pg column (Amersham Biosciences, Buckinghamshire, UK) connected to an ÄKTApurifier UPC-900 system (Amersham Biosciences). RchIL-2 protein was analyzed by SDS-PAGE and Western blot with the anti-His mAb (Amersham Biosciences) as described previously (Zhou et al., 2005a). The monomer of chIL-2 protein was analyzed by native electrophoresis as described previously (Brandhuber et al., 1987) and used in the following experiments. The rchIL-2 monomer was refolded with one-step oxidation procedure as described previously (Wang et al., 2006).

2.3. Production and purification of mAb to chIL-2

The mAbs to chIL-2 were generated using rchIL-2 as an immunogen as performed previously (Chen et al., 2005). To analyze the reactivity of these mAbs against the natural chIL-2 protein, the chIL-2 ORF with the signal peptide sequence was subcloned into the pcDNA3 plasmid (Invitrogen, Carlsbad, CA) according to the manufacturer's instructions. The resulting plasmid, pcDNA3-chIL-2, was transfected into COS-7 cells using Lipofectamine 2000 (Invitrogen) according to the manufacture's instructions. After incubation for 48 h at 37 °C, the cells were washed with PBST and fixed in methanol–acetone mixture (1:1, v/v). Cells were then incubated with mAbs to rchIL-2 followed by HRP-labeled goat anti-mouse-IgG (1:5000, Southern Biotechnology Associates Inc., Birmingham, USA). Color development was carried out with 3-amino-9-ethylcarbazole (BD Pharmingen, San Diego, CA). Subsequently, the mAbs were purified from ascites fluids by caprylic acid/ammonium sulfate precipitation and with a HiTrap Protein G HP column (Amersham Biosciences) connected to an ÄKTApurifier UPC-900 system according to the manufacture's instructions. The mAbs against rchIL-2 were identified by ELISA and Western blot.

2.4. Identification of functional mAbs against chIL-2

The neutralizing activity of the generated mAbs was assayed by the inhibition of chIL-2-stimulated T-cell proliferation. Briefly, 50 μl of rchIL-2 (2 μg/ml) and supernatant of Con A-stimulated SMC were mixed, respectively, with an equal volume of five-fold dilutions of mAbs to chIL-2 protein (5 μg/ml) at 37 °C for 1 h in 96-well plates. The SMC stimulated with Con A for 48 h were incubated in RPMI-1640 medium containing 0.05 mol/L a-methyl-mannoside for 30 min at 37 °C. Dead cells were removed using Lymphoprep (Shanghai Hengxin Chemicals Co. Ltd., Shanghai, China) after centrifugation. Thereafter, 100 μl of live Con A-stimulated SMC (1.5×10^6 cells/ml) was added to each well and the mixture was incubated at 37 °C for 48 h. Proliferation was measured by the WST-8 assay (Cell counting kit-8®, Dojindo, Kumamoto, Japan) according to the manufacturer's instructions. The SMC with rchIL-2 or RPMI-1640 medium were used as positive and negative controls, respectively. The inhibition of cell proliferation was calculated using the following formula: $\text{Inhibition} = (OD_{\text{positive control}} - OD_{\text{sample}})/(OD_{\text{positive control}} - OD_{\text{negative control}}) \times 100\%$.

2.5. Peptide ELISA to determine epitopes with overlapping peptides

Based on the prediction of linear B-cell epitopes defined by BepiPred 1.0 software, fourteen overlapping peptides shifted by seven amino acids, according to chIL-2 sequence

Table 1
Synthetic peptides of the chIL-2 protein.[a].

Peptides	Sequences	Peptides	Sequences
pep1	1 ASLTSAKWKTLQTLIK 16	pep10	80 NLKSLTGLNHTG 91
pep2	10 TLQTLIKDLEILENIK 25	pep11	85 TGLNHTGSECKICEA 99
pep3	19 EILENIKNKIHLELY 33	pep12	93 ECKICEANNKKKF 105
pep4	27 KIHLELYTPTETQEC 41	pep13	99 ANNKKKFPDFLHE 111
pep5	35 PTETQECTQQTLQCYL 50	pep14	105 FPDFLHELTNFVRYLQK 121
pep6	44 QTLQCYLGEVVTLK 57	pep15	27 KIHLELYTPTETQECTQQTL 46
pep7	51 GEVVTLKKETEDDTEI 66	pep16	88NHTGSECKICEANNKKKFPDFLHEL112
pep8	60 TEDDTEIKEEFVTAI 74	pep17	79 KNLKSLTGLNHTGSECKI 96
pep9	68EEFVTAIQNIEKNLKSLTG 86	pepCtrl	FCIFPLTFKSSASPRKFLTNVTGCC

[a] The first and last amino acids in one-letter code and their corresponding positions on chIL-2 are indicated.

(pep1–pep14, Table 1), were synthesized by the solid-phase peptide synthesis method using a Symphony Multiplex Peptide Synthesizer (ProteinTechnologies, Inc., USA). Peptide purities were greater than 90% as assessed by HPLC and mass spectrometry. During synthesis, a cysteine residue was added at the N-terminal of all peptides. Peptides were conjugated to the carrier protein BSA using heterobifunctional cross-linker Sulfo-SMCC (Pierce, USA). These BSA-conjugated peptides were tested for their reactivity with mAbs by ELISA as described below.

Peptide ELISA was performed to analyze the reactivity of peptides with mAbs as described previously (Wang et al., 2005b; Shang et al., 2009). Briefly, microtiter plates (Nunc, Denmark) were coated with 100 μl of 5 μg/ml BSA-conjugated peptide in 0.05 M carbonate buffer (pH 9.6) at 4 °C overnight. The plates were washed and blocked as above. After incubation with 10 μg/mL mAbs at 37 °C for 1 h, the plates were washed five times with TBST (25 mM Tris–HCl, 125 mM NaCl, 0.1% Tween 20, pH 8.0) and incubated with HRP-labeled goat anti-mouse-IgG at 37 °C for 1 h. Following five washes, the colorimetric reaction was developed using TMB chromogenic substrate (Sigma) for 10 min at 37 °C and stopped with 2 M H_2SO_4. The optical density at 450 nm (OD450) was recorded. The carrier protein BSA was included as a negative control.

2.6. Epitope mapping using a phage display random peptide library

Phage display libraries Ph.D.-7 and Ph.D.-12 (NEB, Hertfordshire, UK) were screened by panning according to the manufacturer's instructions. Briefly, 96-well microtiter plates (Nunc) were coated with mAb to chIL-2 at a concentration of 100 mg/L in 0.1 M $NaHCO_3$ (pH 8.6). The mAb-coated wells were blocked with 0.5% BSA in 0.1 M $NaHCO_3$ and washed with 0.5% TBST. For each panning cycle, 2×10^{11} pfu phages were placed in the well and incubated for 1 h. Following the removal of nonbinding phages, bound phages were competitively eluted from the well with 400 μg/ml rchIL-2. The recovered phages were amplified by growing with *E. coli* ER2738 for a new cycle of panning. A total of three or four rounds of selection were performed, and selected phage clones were assayed for binding of mAbs to chIL-2 by a capture ELISA according to the manufacturer's instructions. Ten random selected positive phages were purified from single colonies for DNA sequencing. The consensus mimotope motifs were determined using the aligned amino acid sequences displayed on ten random positive phage clones by Clustal W. The corresponding functional epitopes of mAbs to chIL-2 were subsequently determined through aligning the consensus mimotope motifs with chIL-2, and further overlayed to determine the functional domains of chIL-2. To compare functional domains of chIL-2 with huIL-2, these domains were further aligned with huIL-2.

2.7. Competitive ELISA to identify the native epitope in chIL-2

According to the results of the alignment between the mimotopes and chIL-2, three additional peptides were synthesized as described above (pep15–pep17, Table 1). The epitope peptides, pep9, pep15, pep16, pep17, were used as inhibitors to block the binding of mAbs to rchIL-2 in a competitive ELISA. Microtiter plates were coated with 0.17 μmol/L rchIL-2 in 0.1 mol/L $NaHCO_3$ (pH 8.6) buffer at 4 °C overnight. Monoclonal Abs to chIL-2 at 6.7 nmol/L in 5% skim milk were mixed with an equal volume of inhibitors (8 μmol/L), and pre-incubated for 1 h at 37 °C. Subsequently, mixtures were transferred to the rchIL-2-coated plates at 100 μL/well and the plates were left at 37 °C for 1 h. After washing, HRP-labeled goat anti-mouse-IgG was added and the color developed by TMB. Each dilution was tested in triplicate. BSA and rchIL-2 (8 μmol/L) were used as negative and positive controls, respectively.

2.8. Bioactivity detection of the epitope peptides

Epitope peptides (250 ng/ml) were diluted two-fold and added to the 96-well plates at 100 μl/well, followed by Con A-stimulated T-cells (1.5×10^5 cells/well). RchIL-2 at 1 μg/ml and RPMI-1640 medium were used as positive and negative controls, respectively. An unrelated peptide, pepCtrl (Table 1), was used as a control peptide. After 48 h of incubation, proliferation was measured by the WST-8 assay as described above. The percentage of cell proliferation was calculated using the following formula: $\text{proliferation} = (\text{OD}_{\text{sample}} - \text{OD}_{\text{negative control}})/(\text{OD}_{\text{positive control}} - \text{OD}_{\text{negative control}}) \times 100\%$.

2.9. Construct model of tertiary structures of chIL-2

The tertiary model of chIL-2 protein (GenBank accession no. AF483600) was constructed using SWISS-MODEL workspace server (Arnold et al., 2006). SWISS-MODEL is a fully automated protein structure homology-modeling

server, in which a large sequence database is iteratively searched to construct a sequence profile until a template can be found in a database of proteins with known structure. Query and template sequences are subsequently aligned using a score based on profile–profile comparisons. The program finally constructs the tertiary structure model and provides the file with co-ordinates for model in pdb format. The crystal tertiary drawing of huIL-2 protein was represented with X-ray diffraction as a control (PDB ID code 1PW6B), which was composed of a four-helix bundle (A–D) and two beta sheets (Thanos et al., 2003).

3. Results

3.1. Expression and purification of soluble rchIL-2 protein

Bacterial samples induced by IPTG were ultrasonicated under natural conditions and centrifuged. SDS-PAGE analysis revealed that the bacterial lysate contained His-chIL-2 fusion protein with the predicted molecular weight of 14.8 kDa (Fig. 1, lane 2). The negative bacterial extract did not show the expressed protein band (Fig. 1, lane 1). The rchIL-2 expressed in *E. coli* existed in soluble and insoluble forms (Fig. 1, lanes 3–4). To purify the soluble rchIL-2 protein, nickel affinity was employed under natural conditions. The yield of the eluted soluble protein was approximately 3 mg/L bacterial culture as assessed by the Bradford method (Fig. 1, lane 5). To isolate the rchIL-2 monomer, the soluble product was fractioned using a HiLoad 26/60 Superdex 75 prep pg column. The soluble monomer showed only one form in the SDS-PAGE analysis (Fig. 1, lane 6), but had two forms in the native electrophoresis (Fig. 1, lane 7). The yield of eluted soluble protein monomer was approximately 1 mg/L bacterial culture. The oxidation of four cysteine residues in the purified rchIL-2 monomer was catalyzed by a mixture of reduced and oxidized glutathione following one-step oxidation procedure. The refolded product showed two forms with a little larger molecule in native electrophoresis (Fig. 1, lane 8). In the Western blot analysis, the expressed rchIL-2 could be recognized by anti-His mAb (Fig. 1, lane 9). In contrast, no such band was detected in the lysates of the bacterial cells containing only pET28a(+) (Fig. 1, lane 10).

3.2. Production of functional mAbs to rchIL-2

Thirty-two hybridoma cell lines secreting anti-chIL-2 antibodies were established using the soluble monomer of rchIL-2 (Table S1). The ELISA assay demonstrated that all mAbs had special binding with rchIL-2. Among those mAbs, twenty-five mAbs were IgG1, three were IgG2a, three were IgG2b, and mAb 1E10 was IgM. Immunocytochemistry analysis showed that twelve mAbs could specifically recognize eukaryotic rchIL-2 protein in COS-7 cells, such as mAbs 1E10, 2F9, 2G11, 3E7, 4F3, 6G5, 6H10, 7B7, 7G5, 8H8, 9F2 and 10A4 (Table S1). Furthermore, the neutralizing activities of twelve mAbs were assayed by the inhibition of chIL-2-stimulated T-cell proliferation as described above. Results indicated that lymphocyte proliferations induced by rchIL-2 (Fig. 2) and endogenous chIL-2 (data not shown) were respectively inhibited in a dose-dependent manner by mAbs 2F9, 2G11, 3E7, 4F3, 6H10, 6G5, 7B7, 7G5 and 8H8, but not mAbs 1E10, 9F2 and 10A4. This evidence demonstrates that the anti-chIL-2 mAbs 2F9, 2G11, 3E7, 4F3, 6H10, 6G5, 7B7, 7G5 and 8H8 are neutralizing mAbs.

3.3. Mapping the epitopes of chIL-2 by overlapping peptides

All neutralizing mAbs to chIL-2 were tested for their reactivity with the fourteen overlapping peptides. Peptide

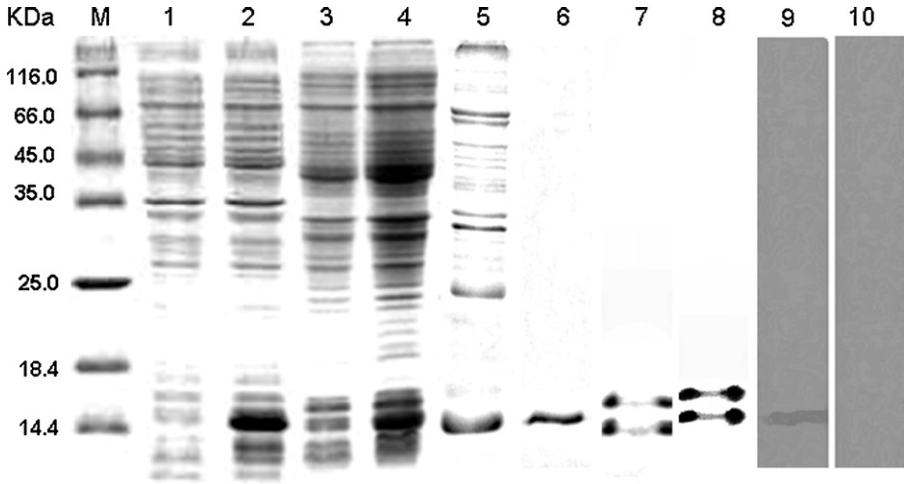

Fig. 1. One-dimensional electrophoresis and Western blot analysis of soluble rchIL-2 expressed in *E. coli* strain BL21 (DE3). Bacteria were ultrasonicated under natural conditions. After centrifugation, the supernatants and pellets were analyzed by SDS-PAGE. Lane M is a molecular weight standard. Lane 1 is the extract of the negative control bacteria containing pET28a(+) vector. Lane 2 is the extract of bacteria transfected with pET28a-chIL-2. Lanes 3 and 4 are supernatants and pellets from bacterial lysates transfected with pET28a-chIL-2 respectively. Lane 5 is the His-rchIL-2 fusion protein purified by the nickel column under native conditions. Lane 6 is the rchIL-2 monomer protein isolated by Gel filtration. Lane 7 is the rchIL-2 monomer protein by native electrophoresis. Lane 8 is the refolded rchIL-2 monomer protein by native electrophoresis. Lane 9 is the rchIL-2 protein recognized by the anti-His mAb. Lane 10 is the extract of the negative control bacteria containing pET28a(+), which does not react with anti-His mAb.

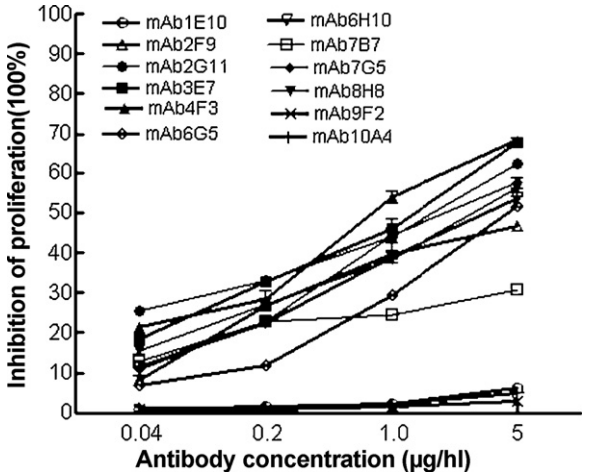

Fig. 2. Neutralizing activity of antibodies against rchIL-2. After serial dilutions, anti-rchIL-2 mAbs were incubated with rchIL-2 protein followed by Con A-stimulated SMC. RchIL-2 (1 μg/mL) and RPMI-1640 medium were respectively used as positive and negative controls. Cell proliferation was measured as described in Section 2. The samples were triplicated, and the experiment was carried out in triplicate. The values are expressed as the means ± S.D.

ELISA analysis showed that most mAbs did not react with the overlapping peptides, indicating that these mAbs did not recognize linear epitopes on chIL-2. Only mAb 2G11 showed a strong reaction with pep9 (P/N = 31) and a weak reaction with pep10 (P/N = 3), but no reaction with pep8 (P/N = 1.1). The results clearly demonstrate that pep9 (E^{68}–T^{86}) is the binding epitope of mAb 2G11 to chIL-2.

3.4. Mimotope motifs of chIL-2 selected by the phage display peptide library

Ten phage clones per mAb were selected from the phage displayed peptide library for all nine anti-chIL-2 neutralizing mAbs. The panning results are summarized in Table 2. The mimotope motifs of nine mAbs were KIELPSL, EHLDXNDSLYL, NHLXGXY, WHLPPSL, EFKASXL, TENPFPE, SGLYL, AHGYWEL and HHGYWEL, respectively. Aligned with chIL-2 by Clustal W, the corresponding putative native epitopes were $K^{27}I^{28}E^{31}L^{32}P^{35}T^{45}L^{46}$, $E^{22}H^{29}L^{30}E^{31}L^{32}Q^{43}Q^{44}T^{45}L^{46}Y^{49}L^{50}$, $N^{26}H^{29}L^{30}E^{31}Q^{47}C^{48}Y^{49}$, $W^{8}H^{29}L^{30}E^{31}P^{35}T^{45}L^{46}$, $E^{69}F^{70}K^{79}K^{82}S^{83}L^{84}L^{87}$, $T^{60}E^{68}N^{88}K^{104}F^{105}P^{106}D^{107}$, $T^{85}G^{86}L^{87}Y^{118}L^{119}$, $N^{88}H^{89}G^{91}F^{105}H^{110}E^{111}L^{112}$ and $N^{88}H^{89}G^{91}F^{105}H^{110}E^{111}L^{112}$, respectively.

Competitive ELISA was performed to identify the putative native epitope peptides that could bind to the mAbs at the antigen-binding site (Fig. 3). The binding of mAbs 2F9, 6G5, 7B7 and 7G5 with chIL-2 was differentially blocked by pep15 (Fig. 3A), and showed that mAbs 2F9, 6G5, 7B7 and 7G5 partially recognized the epitope in pep15 of chIL-2. The binding of mAb 2G11 with chIL-2 was completely blocked by pep9 (Fig. 3A), indicating that pep9 included the intact neutralizing epitope of the chIL-2 protein. This fact strongly supported the specificity of the affinity selection of the phage library and the accuracy of our panning results. Although the deduced native binding epitopes of mAbs 3E7 and 8H8 were partially located in pep16, the binding of mAbs 3E7 and 8H8 with chIL-2 was not blocked by pep16, but differentially blocked by pep8 and pep17, respectively (Fig. 3B), revealing that the efficient binding epitopes of mAbs 3E7 and 8H8 were not in pep16, but in the pep8 and pep17 of chIL-2, respectively. The binding of mAbs 4F3 and 6H10 with chIL-2 was differentially blocked by pep16 (Fig. 3B), revealing that mAbs 4F3 and 6H10 partially recognized the native epitopes in the pep16 of chIL-2. These data confirm that K^{27}–L^{46}, T^{60}–I^{74}, E^{68}–G^{86}, K^{79}–I^{96} and N^{88}–L^{112} constitute the conformational functional epitopes of chIL-2.

However, in a competitive ELISA assay, pep15, pep16 and pep17 had weaker competitive inhibition abilities than rchIL-2, whereas pep8 and pep9 were stronger competitors than chIL-2. We surmise that the integrity of epitope is the major impact factor. Conformational epitopes are discontinuous in sequence and strictly depend on spatial structure and integrity. Peptides corresponding to partial conformational epitopes fail to fold the suitable conformation binding efficiently in an enzyme-linked immunoassay due to their loss of flexibility required for antibody binding. Similar conclusions were confirmed in a previous report (Kim and Pau, 2001).

The efficient binding domains of nine neutralizing epitopes were overlaid with each other by alignment, and three conformational functional domains were displayed (Table 3): $N^{26}K^{27}I^{28}H^{29}L^{30}E^{31}L^{32}P^{35}Q^{43}Q^{44}T^{45}L^{46}Q^{47}$-$C^{48}Y^{49}L^{50}$ (domain I), $E^{68}E^{69}F^{70}K^{79}K^{82}S^{83}L^{84}T^{85}G^{86}L^{87}$ (domain II), and $N^{88}H^{89}G^{91}K^{104}F^{105}P^{106}D^{107}E^{111}$-$L^{112}Y^{118}L^{119}$ (domain III).

3.5. Validation of bioactivity of epitope peptide

The bioactivity of the three functional domains in chIL-2 was further confirmed by the promotion of Con A-stimulated T-cell proliferation. Domain I was mostly positioned in pep15 (K^{27}–L^{46}). Domain II was mostly situated in pep9 (E^{68}–G^{86}). Domain III was mostly distributed in pep16 (N^{88}–L^{112}). Data shown in Fig. 4 indicated that lymphocyte proliferation induced by epitope peptides at a low dosage were significant. However, compared with chIL-2, the proliferation ratio of epitope peptides was low. Pep9 and pep15 induced optimal promotion at 62.5 ng/ml and increased proliferation by 47.14% and 39.78%, respectively. Pep16 had optimal promotion at 250 ng/ml, with an increase in proliferation of 14.08%. The control peptide, pepCtrl, showed no promotion. These data indicate that the three neutralizing epitope peptides of chIL-2 have weak bioactivity and represent functional domains in chIL-2.

3.6. Location of conformational functional domains in tertiary structure of chIL-2

To characterize the relationship between the three functional domains and their structures, tertiary structure of chIL-2 was constructed with the SWISS-MODEL software. Chain A from crystal structure of the IL-15 with IL-15R alpha complex (PDB ID code 2PSMA) was finally used as the template (Olsen et al., 2007). The predicted tertiary structure of mature chIL-2 protein (Fig. 5A), similar to that

Table 2
Alignment of sequences of peptides displayed on the phages isolated and their reactivity with mAbs 7G5, 6G5, 2F9, 7B7, 2G11, 3E7, 8H8, 4F3 and 6H10.

Phage clones	Motif[a]	Phage-displayed peptide sequences	Frequency	OD450[b]
mAb 7G5[c]				
K[27]**I**[28]**E**[31]**L**[32]**P**[35]T[45]**L**[46d]				
Pha7G5	**KIELPSL**	**KIELPSL**	10/10	2.001 ± 0.016
mAb 6G5[e]				
E[22]**H**[29]**L**[30]E[31]L[32]Q[43]Q[44]T[45]**L**[46]**Y**[49]**L**[50f]				
Pha6G5-1	**EHLDXNDSLYL**	**EHLD**WFEDWA**L**W	5/10	0.899 ± 0.157
Pha6G5-2		**EHLD**FL**DS**ENTT	1/10	
Pha6G5-3		**T**YD**ND**M**LY**KNHV	1/10	
Pha6G5-4		F**H**QQNY**NRS**I**YL**	2/10	
Pha6G5-5		**T**GNEKW**LY**GMLT	1/10	
mAb2F[g]				
N[26]**H**[29]**L**[30]E[31]Q[47]C[48]Y[49h]				
Pha2F9-1	**NHLXGXY**	**NHL**N**GS**Y	8/10	0.169 ± 0.041
Pha2F9-2		SI**L**PYP**Y**	1/10	
Pha2F9-3		**NH**KK**G**QQ	1/10	
mAb7B7[i]				
W[8]**H**[29]**L**[30]E[31]**P**[35]T[45]**L**[46j]				
Pha7B7-1	**WHLPPSL**	TY**W**SPT**P**	4/10	1.089 ± 0.844
Pha7B7-2		**WH**VPF**SL**	1/10	
Pha7B7-3		TWA**W**RT**P**	1/10	
Pha7B7-4		**WH**PLL**S**P	1/10	
Pha7B7-5		**WHLP**RVI	1/10	
Pha7B7-6		**WHLP**WLE	1/10	
Pha7B7-7		RNV**PP**M**L**	1/10	
mAb2G11[k]				
E[69]**F**[70]**K**[79]K[82]**S**[83]L[84]**L**[87l]				
Pha2G11-1	**EFKASXL**	YVT**K**IAS	5/10	1.029 ± 0.515
Pha2G11-2		**EF**N**A**AR**L**	2/10	
Pha2G11-3		**EF**NP**S**N**L**	2/10	
Pha2G11-4		**FKAS**LLH	1/10	
mAb 3E7[m]				
T[60]**E**[68]**N**[88]K[104]**F**[105]**P**[106]D[107n]				
Pha3E7-1	**TENPFPE**	YY**NPY**P**E**	1/10	0.699 ± 0.412
Pha3E7-2		**TYNPFPE**	1/10	
Pha3E7-3		QF**NPFPE**	2/10	
Pha3E7-4		W**ENPY**P**E**	2/10	
Pha3E7-5		**TENPFPE**	3/10	
Pha3E7-6		AF**NPFPE**	1/10	
mAb 8H8[o]				
T[85]**G**[86]**L**[87]**Y**[118]**L**[119p]				
Pha8H8-1	**SGLYL**	KI**SGLY**ADLLAK	7/10	0.194 ± 0.029
Pha8H8-2		GP**TGI**D**L**WGAEV	1/10	
Pha8H8-3		**GVYI**NTNRETSS	2/10	
mAb 4F3[q]				
N[88]**H**[89]**G**[91]F[105]H[110]**E**[111]**L**[112r]				
Pha4F3-1	**AHGYWEL**	**AHGYWEL**	10/10	2.509 ± 0.065
mAb 6H10[s]				
N[88]**H**[89]**G**[91]F[105]H[110]**E**[111]**L**[112t]				
Pha6H10-1	**HHGYWEL**	**HHGYWEL**	10/10	0.263 ± 0.134

(a) Alignment of phage-displayed consensus amino acids were shown in boldface to indicate the motifs recognized by mAbs. X represented random amino acid. (b) Binding of selected phages to mAbs by a capture ELISA. BSA was used as a negative control to subtract the background binding. The OD450 was shown as means ± S.D. (c, e, g, i, k, m, o, q, s) Phage clones respectively selected by mAbs 7G5, 6G5, 2F9, 7B7, 2G11, 3E7, 8H8, 4F3 and 6H10. (d, f, h, j, l, n, p, r, t) Predictive native epitopes in chIL-2 were respectively recognized by mAbs 7G5, 6G5, 2F9, 7B7, 2G11, 3E7, 8H8, 4F3 and 6H10, and determined through aligning the consensus mimotope motifs with chIL-2 by Clustal W.

of human IL-2 protein (Fig. 5B), contained typical four-helix bundle structures (Helixes A–D) and two β sheets (Sheets A and B). The length and helix number of four helices of chIL-2 were different from those of the huIL-2 proteins (Table S2). The two β sheets of IL-2, located in the long A–B crossover loop and C–D crossover loop, were spatially adjacent to each other. The length of the β sheets of chIL-2 was different from that of the huIL-2 protein (Table S3). In the model, when the three functional domains of chIL-2 were matched to tertiary structure, domain I was positioned in the long A–B loop, including partial Sheet A, and the N terminal of Helix B. Domain II

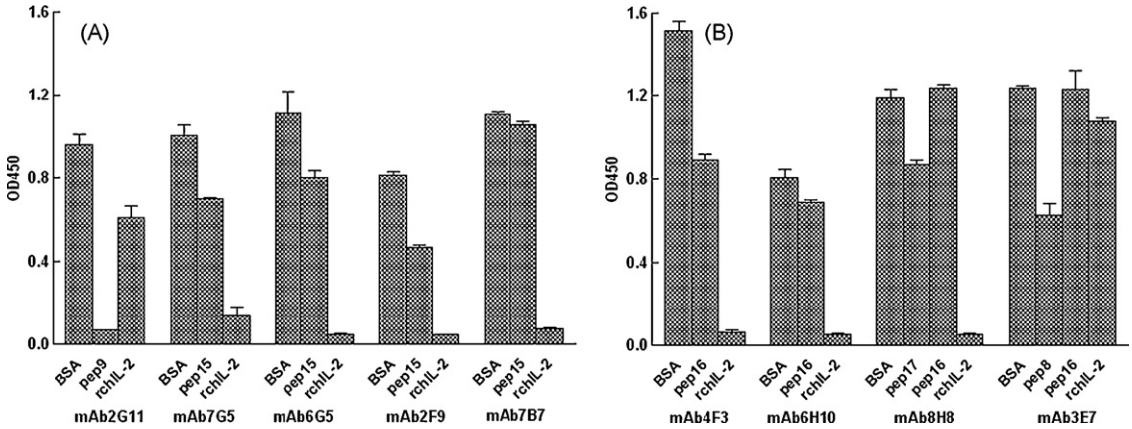

Fig. 3. Effect of synthesized epitope peptides on the binding of mAbs to rchIL-2. (A) The epitope peptides, pep9 and pep15, were used to competitively inhibit the binding of their corresponding mAbs to rchIL-2. (B) The epitope peptides, pep8, pep16 and pep17, were used to competitively inhibit the binding of their corresponding mAbs to rchIL-2. A competitive ELISA was carried out as described in Section 2. Synthesized epitope peptides at 8 μmol/L were used to competitively inhibit the binding of their corresponding mAbs to rchIL-2. BSA and rchIL-2 at 8 μmol/L were included as negative and positive controls, respectively. The samples were triplicated, and the experiment was carried out in triplicate. The values are expressed as the means ± S.D.

Table 3
Alignment of sequences of functional conformational domains in chIL-2 with huIL-2.

Domains	Results of alignment	
Domain I	$N^{26}K^{27}I^{28}$ $H^{29}L^{30}E^{31}L^{32}P^{35}Q^{43}Q^{44}T^{45}L^{46}Q^{47}C^{48}Y^{49}L^{50}$	chIL-2
	$N^{30}K^{35}L^{36}$ $T^{37}F^{42}K^{43}F^{44}P^{47}H^{55}$ – – $L^{56}Q^{57}C^{58}L^{59}E^{60}$	huIL-2
Domain II	$E^{68}E^{69}F^{70}K^{79}K^{82}S^{83}L^{84}T^{85}G^{86}L^{87}$	chIL-2
	$K^{76}N^{77}F^{78}S^{87}N^{90}V^{91}I^{92}V^{93}$ – L^{94}	huIL-2
Domain III	N^{88} $H^{89}G^{91}K^{104}F^{105}P^{106}D^{107}E^{111}L^{112}$ $Y^{118}L^{119}$	chIL-2
	E^{95} L^{96} $G^{98}T^{113}$ I^{114} $V^{115}E^{116}R^{120}W^{121}$ $S^{127}I^{128}$	huIL-2

was mostly situated in Helix C. Domain III was distributed in the C–D loop and Helix D, including partial Sheet B.

4. Discussion

Although several researchers have reported methods for the *in vitro* preparation of rchIL-2 protein (Stepaniak et al., 1999), chIL-2 monomer has not been described. In this experiment, soluble rchIL-2 was produced in *E. coli*, and the rchIL-2 monomer was efficiently isolated with nickel-affinity-Superdex-75-gel-filtration procedure. The rchIL-2 monomer had two forms in native electrophoresis (Fig. 1, lane 7) but displayed only one form in the SDS-PAGE analysis (Fig. 1, lane 6). Refolded rchIL-2 monomer was achieved with one-step oxidation procedure, but still showed two forms in native electrophoresis (Fig. 1, lane 8). This result implies that the rchIL-2 monomer has two isomers in the native conditions, and the isomers are not resulted from different possibilities of disulfide bonds.

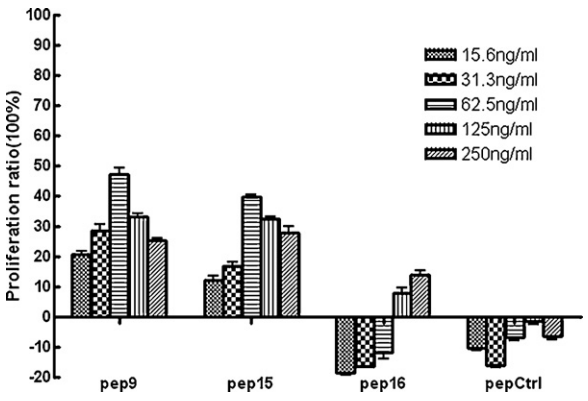

Fig. 4. Proliferation effect of native epitope peptides. After serial dilutions, native epitope peptides were added to the wells followed by Con A-stimulated T-cells. RchIL-2 at 1 μg/ml and RPMI-1640 medium were used as positive and negative controls, respectively. An unrelated peptide, pepCtrl, was used as a control peptide. Cell proliferation was measured by the WST-8 assay. The samples were triplicated, and the experiment was carried out in triplicate. The values are expressed as the means ± S.D.

Until now, there have been no successful efforts to delineate the functional domains of a non-mammalian IL-2 molecule. Epitope mapping has been applied to the understanding of the molecular mechanisms and vaccine design by defining the precise residues present in the structurally or functionally important epitopes (MacCallum et al., 1996). Previous work has determined that chIL-2 expressed in prokaryotic cells could be used to produce the neutralizing mAbs to chIL-2 (Miyamoto et al., 2001; Rothwell et al., 2001). In the present study, nine neutralizing mAbs to chIL-2 were produced using the rchIL-2 monomer. Epitope mapping by synthetic overlapping peptides showed that only mAb 2G11 strongly recognized pep9 (E^{68}–T^{86}). Epitope mapping by two phage display random peptide libraries showed nine mimotope motifs, KIELPSL, EHLDXNDSLYL, NHLXGXY, WHLPPSL, EFKASXL, TENPFPE, SGLYL, AHGYWEL and HHGYWEL,

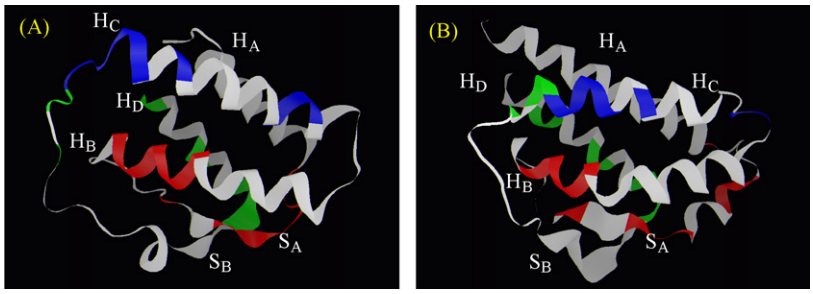

Fig. 5. Predicted three-dimensional structure drawing of chIL-2 with SWISS-MODEL software in ribbon view from the same angle with RasMol software. The functional domain I in chIL-2 and the aligned amino acids in huIL-2 are colored with red. Domain II are colored with blue and domain III are colored with green. (A) Chicken IL-2; (B) crystal structure drawing of human IL-2. H: helix. S: sheet. (For interpretation of the references to color in this figure legend, the reader is referred to the web version of the article.)

were the determinants of antigen recognition by mAbs. When aligning with the sequence of chIL-2, we found the mimotopes are not sequential, further confirming that these mAbs recognize conformational epitopes.

The predicted tertiary structure of chIL-2 contained typical four-helix bundle structures and two β sheets. Clustal W analysis revealed that the identified functional domain I, $N^{26}K^{27}I^{28}H^{29}L^{30}E^{31}L^{32}P^{35}Q^{43}Q^{44}T^{45}L^{46}Q^{47}$-$C^{48}Y^{49}L^{50}$, situated in the A–B loop and the N terminal of Helix B (Fig. 5A) of chIL-2, was aligned with $N^{30}K^{35}L^{36}T^{37}F^{42}K^{43}F^{44}P^{47}H^{55}L^{56}Q^{57}C^{58}L^{59}E^{60}$ in huIL-2 (Fig. 5B), also positioned in the A–B loop and the N terminal of Helix B. Domain I of IL-2 included part of Sheet A (Table S3). Previous reports identified the huIL-2 residues K^{35}, R^{38}, F^{42}, K^{43} and Y^{45} as critical contact sites for binding to the IL-2R alpha chain (Sauve et al., 1991; Wang et al., 2005a,b). The data reported in this study suggests that conformational functional domain I in chIL-2 binds the chIL-2R alpha chain, and residues K^{27}, L^{30} and E^{31} could be the critical contact sites. The identified functional domain II ($E^{68}E^{69}F^{70}K^{79}K^{82}S^{83}L^{84}T^{85}G^{86}L^{87}$) was included in Helix C (Fig. 5A). The aligned sequence in huIL-2, $K^{76}N^{77}F^{78}S^{87}N^{90}V^{91}I^{92}V^{93}L^{94}$, was also positioned in Helix C (Fig. 5B). N^{88} of huIL-2 is critical for IL-2R beta binding by mutagenesis analysis (Shanafelt et al., 2000). Amino acid N^{80} of chIL-2, aligned with N^{88} of huIL-2, was not included in domain II. We surmise that the function of N^{80} in chIL-2 is to maintain the conformation, thereby allowing the binding of the chIL-2R beta chain with domain II. The identified functional domain III ($N^{88}H^{89}G^{91}K^{104}$ $F^{105}P^{106}D^{107}E^{111}L^{112}Y^{118}L^{119}$) in chIL-2 was aligned with $E^{95}L^{96}G^{98}T^{113}I^{114}V^{115}E^{116}R^{120}W^{121}S^{127}I^{128}$ in huIL-2, locating around the conserved residues, F^{117} and L^{118}, in huIL-2. Recent crystallography studies confirm that residues around conserved residues, F^{117} and L^{118}, in huIL-2 are the contact sites for the huIL-2R gamma chain (Wang et al., 2005a). Our results suggest that domain III was one of the conformational functional domains deduced to bind the chIL-2R gamma chain.

The potential important amino acids in the function of chIL-2 are now in progress to be confirmed by mutational analysis. The work described in this study advances our understanding of the structure–function relationship of chIL-2 and provides a clue for improving the activity of chIL-2 through molecular design.

Acknowledgements

This work was supported by grants from National Science Foundation of China (Grant Nos. 30625030 and 30771589), and supported by the earmarked fund for Modern Agro-industry Technology Research System.

Appendix A. Supplementary data

Supplementary data associated with this article can be found, in the online version, at doi:10.1016/j.vetimm.2009.10.021.

References

Arnold, K., Bordoli, L., Kopp, J., Schwede, T., 2006. The SWISS-MODEL Workspace: a web-based environment for protein structure homology modelling. Bioinformatics 22, 195–201.

Buchli, P., Ciardelli, T., 1993. Structural and biologic properties of a human aspartic acid-126 interleukin-2 analog. Arch. Biochem. Biophys. 307, 411–415.

Brandhuber, B.J., Boone, T., Kenney, W.C., McKay, D.B., 1987. Three-dimensional structure of interleukin-2. Science 238, 1707–1709.

Chen, J.G., Chen, W.H., Zhou, J.Y., Wang, J.Y., Qi, J., Zheng, X.J., Yu, Z.Z., 2005. In vitro expression and bioactivity of chicken interleukin-2. Scientia Agricult. Sin. 38, 1034–1039.

Choi, K.D., Lillehoj, H.S., 2000. Role of chicken IL-2 on γδ T-cells and *Eimeria acervulina*-induced changes in intestinal IL-2 mRNA expression and γδ T-cells. Vet. Immunol. Immunopathol. 73, 309–321.

Collins, L., Tsien, W.H., Seals, C., Hakimi, J., Weber, D., Bailon, P., Hoskings, J., Greene, W.C., Toome, V., Ju, G., 1988. Identification of specific residues of human interleukin-2 that affect binding to the 70-kDa subunit (p70) of the interleukin-2 receptor. Proc. Natl. Acad. Sci. U.S.A. 85, 7709–7713.

Eckenberg, R., Xu, D., Moreau, J.L., Bossus, M., Mazie, J.C., Tartar, A., Liu, X.Y., Alzari, P.M., Bertoglio, J., Theze, J., 1997. Analysis of human IL-2/IL-2 receptor beta chain interactions: monoclonal antibody H2-8 and new IL-2 mutants define the critical role of alpha helix-A of IL-2. Cytokine 9, 488–498.

Farner, N., Hank, J., Sondel, P., 1997. Interleukin-2: molecular and clinical aspects. In: Remick, D.G., Friedland, J.S. (Eds.), Cytokines in Health and Disease. M. Dekker, Inc., New York, pp. 29–40.

Gu, J.Y., Teng, Q.Y., Huang, Z.Y., Zhou, J.Y., 2007. Transcription analysis and prokaryotic expression of chicken IL-2 receptor gamma chain gene. Vet. Sci. China 37, 71–77.

Hilton, L.S., Bean, A.G., Kimpton, W.G., Lowenthal, J.W., 2002. Interleukin-2 directly induces activation and proliferation of chicken T cells in vivo. J. Interferon. Cytokin. Res. 22, 755–763.

Hulse, D.J., Romero, C.H., 2004. Partial protection against infectious bursal disease virus through DNA-mediated vaccination with the VP2 capsid protein and chicken IL-2 genes. Vaccine 22, 1249–1259.

Ju, G., Collins, L., Kaffka, K.L., Tsien, W.H., Chizzonite, R., Crowl, R., Bhatt, R., Kilian, P.L., 1987. Structure-function analysis of human interleukin-2.

Identification of amino acid residues required for biological activity. J. Biol. Chem. 262, 5723–5731.
Kim, P., Pau, C.P., 2001. Comparing tandem repeats and multiple antigenic peptides as the antigens to detect antibodies by enzyme immunoassay. J. Immunol. Methods 257, 51–54.
MacCallum, R.M., Martin, A.C., Thornton, J.M., 1996. Antibody–antigen interactions: contact analysis and binding site topography. J. Mol. Biol. 262, 732–745.
Miyamoto, T., Lillehoj, H.S., Sohn, E.J., Min, W., 2001. Production and characterization of monoclonal antibodies detecting chicken interleukin-2 and the development of an antigen capture enzyme-linked immunosorbent assay. Vet. Immunol. Immunopathol. 80, 245–257.
Olsen, S.K., Ota, N., Kishishita, S., Kukimoto-Niino, M., Murayama, K., Uchiyama, H., Toyama, M., Terada, T., Shirouzu, M., Kanagawa, O., Yokoyama, S., 2007. Crystal structure of the interleukin-15.interleukin-15 receptor alpha complex: insights into trans and cis presentation. J. Biol. Chem. 282, 37191–37204.
Rothwell, L., Hamblin, A., Kaiser, P., 2001. Production and characterisation of monoclonal antibodies specific for chicken interleukin-2. Vet. Immunol. Immunopathol. 83, 149–160.
Rubin, J.T., 1995. Interleukin-2: its rational and role in the treatment of patients with cancer. Cancer Treat. Res. 80, 83–105.
Sauve, K., Nachman, M., Spence, C., Bailon, P., Campbell, E., Tsien, W.H., Kondas, J.A., Hakimi, J., Ju, G., 1991. Localization in human interleukin-2 of the binding site to the alpha chain (p55) of the interleukin-2 receptor. Proc. Natl. Acad. Sci. U.S.A. 88, 4636–4640.
Shanafelt, A.B., Lin, Y., Shanafelt, M.-C., Forte, C.P., Dubois-Stringfellow, N., Carter, C., Gibbons, J.A., Cheng, S.L., Delaria, K.A., Fleischer, R., Greve, J.M., Gundel, R., Harris, K., Kelly, R., Koh, B., Li, Y., Lantz, L., Mak, P., Neyer, L., Plym, M.J., Roczniak, S., Serban, D., Thrift, J., Tsuchiyama, L., Wetzel, M., Wong, M., Zolotorev, A., 2000. A T-cell selective interleukin-2 mutein exhibits potent antitumor activity and is well tolerated in vivo. Nat. Biotech. 18, 1197–1202.
Shang, S.B., Jin, Y.L., Jiang, X.T., Zhou, J.Y., Zhang, X., Xing, G., He, J.L., Yan, Y., 2009. Fine mapping of antigenic epitopes on capsid proteins of porcine circovirus, and antigenic phenotype of porcine circovirus Type 2. Mol. Immunol. 46, 327–334.
Stepaniak, J.A., Shuster, J.E., Hu, W., Sundick, R.S., 1999. Production and in vitro characterization of recombinant chicken interleukin-2. J. Interferon Cytokine Res. 19, 515–526.
Sundick, R.S., Gill-Dixon, C., 1997. A cloned chicken lymphokine homologous to both mammalian IL-2 and IL-15. J. Immunol. 159, 720–725.
Thanos, C.D., Randal, M., Wells, J.A., 2003. Potent small-molecule binding to a dynamic hot spot on IL-2. J. Am. Chem. Soc. 125, 15280–15281.
Teng, Q.Y., Zhou, J.Y., Wu, J.J., Guo, J.Q., Shen, H.G., 2006. Characterization of chicken interleukin 2 receptor alpha chain, a homolog to mammalian CD25. FEBS Lett. 580, 4274–4281.
Wang, J.Y., Fang, J., Guo, J.Q., Teng, Q.Y., Huang, Z.Y., Gu, J.Y., Shen, H.G., Zhou, J.Y., 2007. Molecular cloning and characterization of Duck CD25. Vet. Immunol. Immunopathol. 117, 266–274.
Wang, J., Qi, J., Shen, H., Zhou, J., Fang, J., Chen, H., Wang, Z., Li, H., 2006. In vivo CD4+ T-cell up-regulation and high dose side effects of refolded duck interleukin-2. Cytokine 34, 297–302.
Wang, X., Rickert, M., Garcia, K.C., 2005a. Structure of the quaternary complex of interleukin-2 with its alpha, beta, and gammac receptors. Science 310, 1159–1163.
Wang, X.N., Zhang, G.P., Zhou, J.Y., Feng, C.H., Yang, Y.Y., Li, Q.M., Guo, J.Q., Qiao, H.X., Xi, J., Zhao, D., Xing, G.X., Wang, Z.L., Wang, S.H., Xiao, Z.J., Li, X.W., Deng, R.G., 2005b. Identification of neutralizing epitopes on the VP2 protein of infectious bursal disease virus by phage-displayed heptapeptide library screening and synthetic peptide mapping. Viral Immunol. 18, 549–557.
Xu, Q., Song, X., Xu, L., Yan, R., Shah, M.A., Li, X., 2008. Vaccination of chickens with a chimeric DNA vaccine encoding *Eimeria tenella* TA4 and chicken IL-2 induces protective immunity against coccidiosis. Vet. Parasitol. 156, 319–323.
Zhou, J.Y., Chen, J.G., Wang, J.Y., Kwang, J., 2003. Cloning and genetic evolution analysis of chIL-2 gene of Chinese local breeds. Prog. Biochem. Biophys. 30, 384–389.
Zhou, J.Y., Wang, J.Y., Chen, J.G., Wu, J.X., Gong, H., Teng, Q.Y., Guo, J.Q., Shen, H.G., 2005a. Cloning, in vitro expression and bioactivity of duck interleukin-2. Mol. Immunol. 42, 589–598.
Zhou, J.Y., Chen, J.Y., Wang, J.Y., Wu, J.X., Gong, H., Chen, Q.J., 2005b. cDNA cloning and functional analysis of goose interleukin-2. Cytokine 30, 328–338.
Zurawski, S.M., Mosmann, T.R., Benedik, M., Zurawski, G., 1986. Alterations in the amino-terminal third of mouse interleukin-2: effects on biological activity and immunoreactivity. J. Immunol. 137, 3354–3360.